Theoretical investigation of the phonon spectrum and the lattice thermal conductivity in GeTe.

© D.A. Pshenay-Severin, A.A. Shabaldin, P.P. Konstantinov, A.T. Burkov

Ioffe Institute,
194021 St. Petersburg, Russia
E-mail: d.pshenay@mail.ru

Received August 12, 2021
Revised August 28, 2021
Accepted August 28, 2021

Recently, there has been renewed interest in thermoelectric materials based on germanium telluride, which demonstrate high efficiency in mid-temperature range. This paper discusses the theoretical description of the phonon spectrum and lattice thermal conductivity in GeTe using ab initio methods. Using these methods, the temperature dependence of the lattice thermal conductivity in the rhombohedral phase was calculated and effects of scattering by point defects and nanostructuring were estimated. The modification of the phonon spectrum upon the transition to the high-temperature cubic phase is investigated. The calculated temperature dependences of the lattice thermal conductivity are compared with the available experimental data on GeTe and its solid solutions.

Keywords: germanium telluride, ab initio calculations, phonon spectrum, lattice thermal conductivity, nanostructuring.

DOI: 10.21883/SC.2022.14.53854.12

1. Introduction

Germanium telluride is a promising medium-temperature thermoelectric material. GeTe itself and its solid solutions with PbTe feature high thermoelectric efficiency values [1–5]. The concentration of lead in them is low, which is ecologically appealing. Pure GeTe features a high density of germanium vacancies and, consequently, a high hole density [6]. Doping with bismuth and antimony was used to optimize the hole density in GeTe and in solid solutions with PbTe [1–5]. The value of ZT in $Ge_{0.95}Pb_{0.05}Te$ solid solutions doped with bismuth is as high as 1.5, while undoped solutions of this composition have $ZT \leq 1.1$ [1,2]. The values of parameter ZT achieved in recent studies of $Ge_{0.9}Pb_{0.1}Te$ solid solutions doped with bismuth and antimony were well above 2 [3,4]. Lead-free samples with added indium and antimony had $ZT = 2.3$ [5].

It is clear that materials with their thermoelectric efficiency being this high are well-suited for use in thermoelectric generators. However, these experimental results require independent verification. It is also important to determine which features of the electronic structure and the phonon spectra of GeTe-based materials define their high thermoelectric efficiency, since this should help find the ways to enhance it further.

Ab initio methods for calculation of electron and phonon spectra and transport have enjoyed rapid progress in recent years. In the present study, the results of calculations of lattice properties of GeTe in the low-temperature rhombohedral α phase are reported, and the phonon spectrum modification in the high-temperature cubic β phase is considered. The obtained results are compared with the available literature data; the accuracy of theoretical description of experimental temperature dependences of the thermal conductivity is analyzed, and the probable reasons why theoretical data deviate from experimental ones are identified.

2. Phonon spectrum and lattice thermal conductivity in the rhombohedral GeTe phase

A considerable number of studies focused on ab initio calculations of the electronic band structure and the phonon spectrum in the low-temperature rhombohedral GeTe phase have already been published. Structural and electronic properties have been investigated in normal conditions [7] and under pressure [8]. Elastic and dielectric properties and the phonon spectrum of GeTe have been calculated, the influence of emerging soft phonon modes on the phase transition from the low-temperature rhombohedral α phase to the high-temperature cubic phase has been examined, and the lattice thermal conductivity in the α phase has been calculated [9–12].

In the present study, calculations were performed in VASP [13,14] in the scalar relativistic approximation. A cutoff energy of 250 eV and a $12 \times 12 \times 12$ Monkhorst–Pack grid were used. The theoretical equilibrium values of lattice parameters of α-GeTe (space group $R3m$, No. 160) turned out be equal to $a = 4.3717$ Å and $\alpha = 57.89°$. A Ge atom was positioned at the origin of coordinates, and a Te atom was in position (x, x, x), $x = 0.47$ in crystal coordinates. In addition, Born charges (3.4 and 5.4 along the trigonal axis and perpendicular to it, respectively) and the high-frequency permittivity (35.1 and 39.5) were calculated with the application of density functional perturbation theory.

The phonon spectrum and the lattice thermal conductivity were calculated in Phono3Py [16,17] using the method of finite displacements in a supercell. The second- and third-order force constants were calculated in a rhombohedral $4 \times 4 \times 4$ supercell with an interaction radius up to 6.4 Å for third-order force constants. The lattice thermal conductivity was calculated with account for three-phonon scattering processes in the relaxation-time approximation; integration over the Brillouin zone was performed on a $27 \times 27 \times 27$ grid. The obtained phonon spectrum is presented in Fig. 1. The lattice parameters listed above and the spectrum agree well with those reported in [11,12,18].

The results of calculation of the lattice thermal conductivity and the experimental data from [1,3,15] are compared in Fig. 2. The experimental lattice thermal conductivity value was calculated from the overall thermal conductivity using the Wiedemann–Franz law with a Lorentz number determined with the help of the formula proposed in [19] and experimental values of thermopower. The use of thermopower data in calculation of the Lorentz number allows one to introduce the carrier degeneracy into analysis. The calculation for pure GeTe yielded $\kappa_{ph} = 3.2$ W/mK at room temperature (curve *1′* in Fig. 2), while the experimental value is 2.5 W/mK. Substitution atoms and vacancies present in the sample give rise to an additional mechanism of scattering on point defects. Its intensity depends on atomic fraction f_i of substitution atoms, ratio $(\Delta M_i/\overline{M})^2$ of the mass difference of substitution atoms to the mean mass of atoms, and the degree of lattice deformation around a substitution atom [20]. One may neglect all factors except the mass difference and thus obtain a rough upper-bound estimate of the lattice thermal conductivity in the presence of point defects; the scattering intensity is then proportional to $f_M = \sum_i f_i(\Delta M_i/\overline{M})^2$. If the scattering off Ge vacancies with a density of 1.5 at%, which corresponds to a hole density of $5 \cdot 10^{20}$ cm^{-3}, is taken into account in such a way, the results of calculations agree more closely with the experimental data (curve *1″* in Fig. 2). Similar calculations performed in [12] yielded lattice thermal conductivities in the range of 2.6–3.2 W/mK for pure GeTe (depending on the type of the density functional approximation used). In the case with 3 at% of Ge vacancies present, these calculations predicted a more than twofold reduction in κ_{ph} at room temperature. To put this into perspective, the same vacancy density in our calculations corresponds to a 1.6-fold κ_{ph} reduction. Figure 2 shows the results of similar calculations for $Ge_{0.96}Bi_{0.04}Te$ (*2, 2′*) and $Ge_{0.91}Bi_{0.04}Pb_{0.05}Te$ (curves *3, 3′*) solid solutions. They agree fairly closely with the experimental data from [1]. A reduction in thermal conductivity is evident; coupled with the hole density optimization, it has a positive effect on the thermoelectric figure of merit. The dependences of κ_{ph} on f_M at 330 K in comparison with the experimental values for several samples from [1,3,15] are shown in the inset of Fig. 2. The calculated curve provides a generally accurate description of the reduction in lattice thermal conductivity induced by an increased impurity density and a more intense

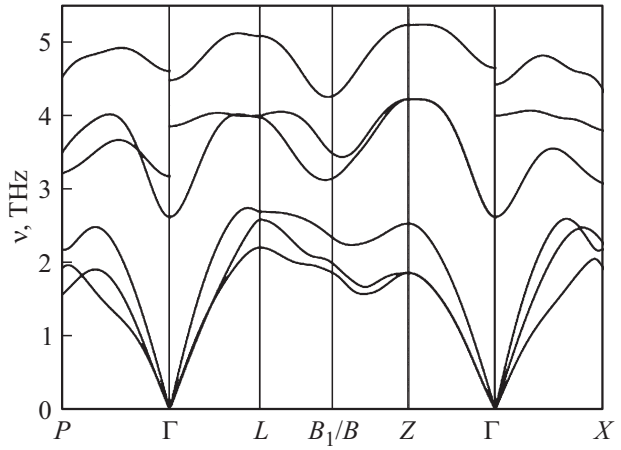

Figure 1. Phonon spectrum of the rhombohedral GeTe phase.

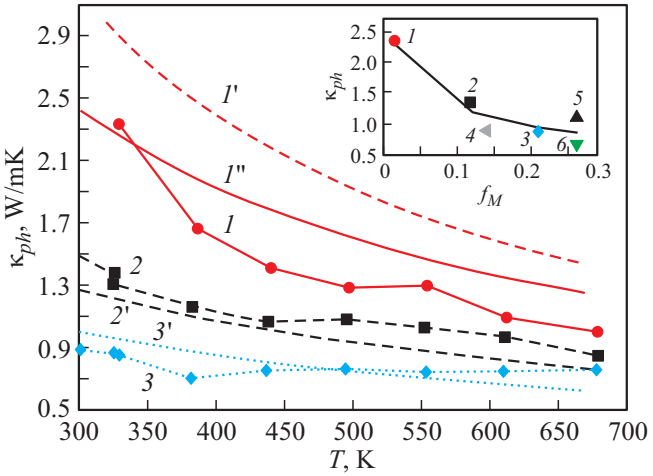

Figure 2. Temperature dependences of lattice thermal conductivity κ_{ph}. The dependences of κ_{ph} on mass-difference scattering factor f_M at 330 K are presented in the inset. *1–4* — experimental data from [1] space (*1*), $Ge_{0.96}Bi_{0.04}Te$ (*2*), $Ge_{0.91}Bi_{0.04}Pb_{0.05}Te$ (*3*), $Ge_{0.95}Pb_{0.05}Te$ (*4*); *5* — $Ge_{0.86}Bi_{0.04}Pb_{0.1}Te$ [15]; *6* — $Ge_{0.86}Bi_{0.04}Pb_{0.1}Te$ [3]. *1′* and *1″* — calculated data for GeTe without and with account for Ge vacancies; *2′* and *3′* — calculated data for the corresponding solid solutions.

scattering off point defects, although the experimental and calculated data for samples *4–6* agree somewhat less closely. This may be attributed to the scatter of experimental data and to the fact that the effects of lattice deformation around a defect were neglected in calculations. One may estimate the influence of nanostructuring on κ_{ph} using the obtained data on phonon relaxation time. Cumulative lattice thermal conductivity κ_{cum}, which characterizes the contribution of phonons with a mean free path shorter than l_{ph} to the thermal conductivity, is convenient for this purpose. This quantity is presented in Fig. 3. The scattering on grain boundaries with size L should reduce the contribution of phonons with $l_{ph} > L$ to the thermal conductivity.

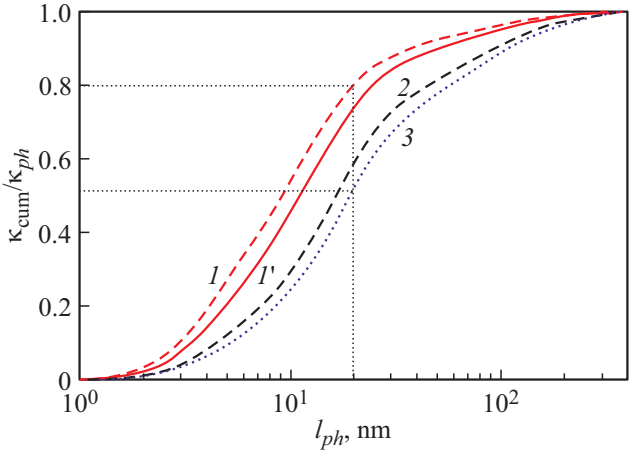

Figure 3. Dependence of the cumulative lattice thermal conductivity on phonons mean free path at room temperature for GeTe without (*1*) and with (*1′*) account for Ge vacancies, $Ge_{0.96}Bi_{0.04}Te$ (*2*), and $Ge_{0.91}Bi_{0.04}Pb_{0.05}Te$ (*3*).

For example, the thermal conductivity in GeTe and solid solutions based on it is expected to decrease by 20% and up to 50%, respectively, at room temperature in the case of 20 nm-sized grains. This corroborates the conclusions drawn in [21] that the processes of scattering on point defects and boundaries reach their maximum efficiency in different phonon wavelength ranges and complement each other, inducing a reduction in thermal conductivity that is more significant in solid solutions than in a pure crystal. A similar calculation for 600 K yielded a 10–20% weaker reduction, since the mean free path decreases at higher temperatures. Although the electron contribution to thermal conductivity in GeTe samples is almost 2 times higher than the lattice one, these contributions become comparable in solid solutions, and ZT is expected to increase due to boundary scattering. For example, the $Ge_{0.91}Bi_{0.04}Pb_{0.05}Te$ sample has $\kappa_h = 1.1$ W/mK and $\kappa_{ph} = 0.86$ W/mK. With the hole contribution being constant and the lattice part reduced by 50%, the overall thermal conductivity should decrease by 20%. If the thermopower and the electric conductivity remain unchanged, this should translate into a corresponding increase in ZT.

3. Phonon spectrum in the high-temperature cubic GeTe phase

The phase transition from the rhombohedral structure to the cubic one in GeTe occurs at a temperature of 638–703 K [22]. The phonon spectrum calculation procedure used above for α-GeTe is inapplicable in this case. The problem is that density functional calculations, which yield interatomic interaction forces, correspond to zero temperature, and the cubic GeTe modification is unstable at zero temperature. Therefore, atomic displacements corresponding to the rhombohedral distortion of the cubic structure result in energy reduction. This gives rise to negative values of squares of phonon frequencies for the corresponding modes (or imaginary frequencies, which are often represented conventionally by negative numbers in the phonon spectrum). The influence of soft phonon modes on the phase transition has been discussed in detail in [11]. The results of calculation of the phonon spectrum for β-GeTe with theoretical equilibrium lattice parameter $a = 6.014$ Å are shown in Fig. 4 (left panel) for illustrative purposes. It can be seen that imaginary phonon modes are present at Γ and X points. Small-magnitude imaginary modes at the Γ point correspond to optical oscillations with Ge and Te atoms shifting in opposite directions. This is consistent with the rhombohedral lattice distortion.

Anharmonic corrections to the spectrum need to be taken into account to perform an accurate calculation of the phonon spectrum in the cubic phase. This calculation turns out to be considerably more demanding. In the present study, the temperature-dependent effective potential (TDEP) method [23,24] was used in calculations. The potential energy in the TDEP method expands into a series in terms of atomic displacements, but the expansion coefficients depend on temperature. They are determined by performing molecular dynamics (MD) simulations of the motion of atoms in a crystal at a given temperature. At each simulation step, the values of atomic displacements and interatomic interaction forces are retained. Second-order and higher-order effective force constants are determined using the least-squares method based on the MD calculation data. An effective harmonic approximation (or a higher-order approximation) is obtained this way for the potential energy at a given temperature. The obtained effective force constants provide an opportunity to use lattice dynamics methods to plot the phonon spectrum and calculate the lattice thermal conductivity.

MD calculations were performed in VASP in an NVT ensemble. X-ray diffraction data for GeTe from [6] were used to determine the temperature of the phase transition and the lattice parameters. The transition to the cubic phase occurred above 640 K, and the lattice constant increased and reached $a = 6.022$ Å [6] at 750 K (the highest studied temperature). This lattice constant value was used in the calculation, which was also carried out at 750 K. The calculation was performed for a $4 \times 4 \times 4$ (128 atoms) supercell, the cutoff energy was 250 eV, and the Monkhorst–Pack grid in the Brillouin zone of the supercell was $2 \times 2 \times 2$. The integration step for equations of motion was 1 fs; a total of 7000 steps were simulated. Using these data and the TDEP code [23,24], we calculated the second- and third-order effective force constants for the mentioned temperature.

The obtained phonon spectrum in the cubic GeTe phase is shown in Fig. 4 (right panel). The stabilization of imaginary phonon modes at high temperatures is evident. The spectrum agrees with the one presented in [25], where an alternative approach was used and calculations were performed at 800 K with a theoretical equilibrium (at

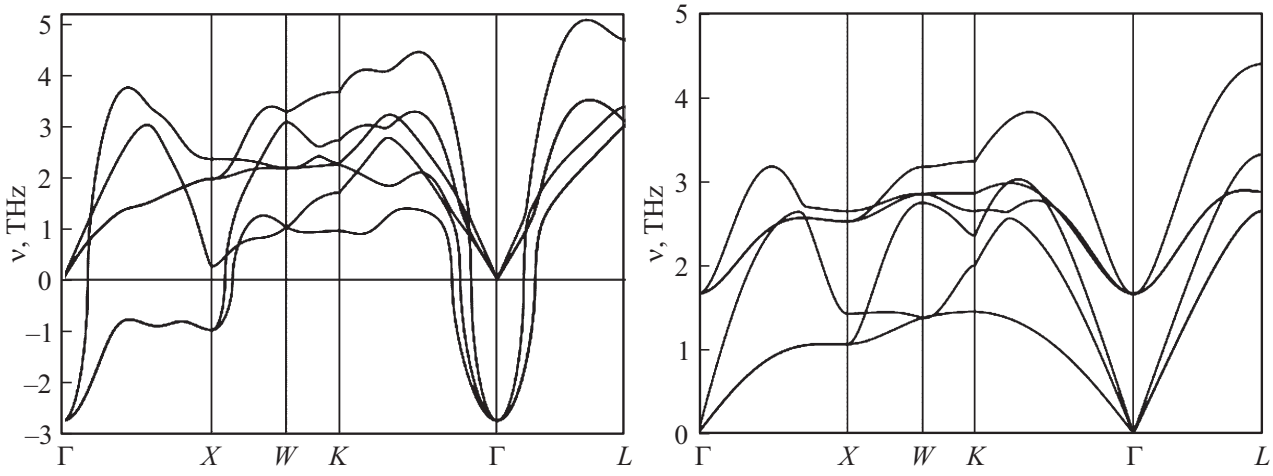

Figure 4. Phonon spectrum calculated in the cubic β phase of GeTe at 0 K (left) and at 750 K (right).

zero temperature) lattice constant of 6.014 Å. An iterative algorithm was used to calculate the force constants in [25]. This calculation started with the force constant values at 0 K. A set of atomic displacements for this temperature was generated based on the effective harmonic approximation using the initial values of force constants, and the corresponding interatomic forces were calculated. These data were then used to find new effective force constants, and the cycle was repeated until convergence was achieved.

The lattice thermal conductivity in the cubic GeTe phase was calculated using the TDEP code based on the obtained second- and third-order force constants. It follows from the comparison with the experimental lattice thermal conductivity of GeTe ($\sim 1.36-1.44$ W/mK at 800 K [25]) that the calculated value (~ 4 W/mK) is ~ 2.6 times higher. A similar calculated value of 3.8 W/mK was obtained in [25]. As was demonstrated in [25], the deviation of theoretical values from experimental ones is attributable to the fact that only three-phonon scattering processes were taken into account in calculations. When four-phonon processes were introduced, the calculated thermal conductivity decreased by $\sim 55\%$ and agreed well with the experimental data. At the same time, the scattering on Ge vacancies at high temperatures is not that efficient. At a vacancy density of 2.1 at% ($p_h = 7.8 \cdot 10^{20}$ cm^{-3}), it helped reduce the thermal conductivity from 1.7 to 1.5 W/mK, thus minimizing the gap between theoretical and experimental data [25]. Since such calculations are very resource-intensive, four-phonon scattering processes were not taken into account in the present study.

4. Conclusion

Thus, using literature data and our own calculations, we illustrated the extent to which modern ab initio methods of characterization of the phonon spectrum and the lattice thermal conductivity are applicable to such a complex object as germanium telluride. The complexity of its theoretical characterization stems from a change in the crystal structure and the phonon spectrum occurring in a phase transition from the rhombohedral phase to the cubic one and from the high hole density (due to the presence of Ge vacancies).

The results of calculation of lattice thermal conductivity α-GeTe with the scattering on germanium vacancies taken into account agreed fairly closely with the experimental data and provided an opportunity to estimate the thermal conductivity reduction in the case of scattering off point substitutional defects (Pb and Bi). A closer fit between calculated and experimental values for solid solutions with Ge substituted with Pb or Bi may be obtained by characterizing more accurately the influence of modification of the phonon spectrum and the phonon lifetime in solid solutions. Such calculation techniques are now being developed extensively (see, e.g., review [26]). The examination of influence of scattering off grain boundaries on κ_{ph} revealed that the lattice thermal conductivity may decrease by up to 20% in pure GeTe and by up to 50% in solid solutions at room temperature if the grain size is 20 nm. The thermal conductivity reduction at higher temperatures is less significant.

The characterization of properties of the high-temperature β phase of GeTe presents the most difficulties, since common density functional calculations correspond to zero temperature and do not provide a correct description of the phonon spectrum. Since direct non-equilibrium ab initio MD methods are too resource-intensive, the temperature-dependent effective potential method was used. The stabilization of soft phonon modes through the effective introduction of anharmonicity allows one to obtain a phonon spectrum and calculate the thermal conductivity using the methods of lattice dynamics. Four-phonon scattering processes need to be taken into account in the process to produce a correct description of the lattice thermal conductivity.

Funding

This study was supported by the Russian Foundation for Basic Research, grant No. 18-52-80005 (BRICS).

Conflict of interest

The authors declare that they have no conflict of interest.

References

[1] L.V. Prokofieva, Yu.I. Ravich, D.A. Pshenay-Severin, P.P. Konstantinov, A.A. Shabaldin. Semiconductors, **46**, 866 (2012).
[2] T. Parashchuk, A. Shabaldin, O. Cherniushok, P. Konstantinov, I. Horichok, A. Burkov, Z. Dashevsky. Physica B: Condens. Matter, **596**, 412397 (2020).
[3] J. Li, X. Zhang, Z. Chen, S. Lin, W. Li, J. Shen, I.T. Witting, A. Faghaninia, Y. Chen, A. Jain, L. Chen, G.J. Snyder, Y. Pei. Joule, **2**, 976 (2018).
[4] J. Li, X. Zhang, X. Wang, Z. Bu, L. Zheng, B. Zhou, F. Xiong, Y. Chen, Y. Pei. J. Am. Chem. Soc., **140**, 16190 (2018).
[5] M. Hong, Z.-G. Chen, L. Yang, Y.-C. Zou, M.S. Dargusch, H. Wang, J. Zou. Adv. Mater., **30**, 1705942 (2018).
[6] E.M. Levin, M.F. Besser, R. Hanus. J. Appl. Phys., **114**, 83713 (2013).
[7] K.M. Rabe, J.D. Joannopoulos. Phys. Rev. B, **36**, 3319 (1987).
[8] A. Ciucivara, B.R. Sahu, L. Kleinman. Phys. Rev. B, **73**, 214105 (2006).
[9] R. Shaltaf, X. Gonze, M. Cardona, R.K. Kremer, G. Siegle. Phys. Rev. B, **79**, 075204 (2009).
[10] R. Shaltaf, E. Durgun, J.-Y. Raty, Ph. Ghosez, X. Gonze. Phys. Rev. B, **78**, 205203 (2008).
[11] U.D. Wdowik, K. Parlinski, S. Rols, T. Chatterji. Phys. Rev. B, **89**, 224306 (2014).
[12] D. Campi, L. Paulatto, G. Fugallo, F. Mauri, M. Bernasconi. Phys. Rev. B, **95**, 024311 (2017).
[13] G. Kresse, D. Joubert. Phys. Rev. B, **59**, 1758 (1999).
[14] G. Kresse, J. Furthmüller. Phys. Rev. B, **54**, 11169 (1996).
[15] A.A. Shabaldin, P.P. Konstantinov, A.Y. Samunin. *XVII Int. Conf. Thermoelectrics and Their Applications* (ISCTA 2021), St. Petersburg, Russia, September 13–16, 2021.
[16] A. Togo, L. Chaput, I. Tanaka. Physical Review B **91**, 094306 (2015).
[17] K. Mizokami, A. Togo, I. Tanaka. Phys. Rev. B, **97**, 224306 (2018).
[18] V. Askarpour, J. Maassen. Phys. Rev. B, **100**, 075201 (2019).
[19] H.-S. Kim, Z.M. Gibbs, Y. Tang, H. Wang, G.J. Snyder. APL Materials, **3**, 41506 (2015).
[20] P.G. Klemens. Proceedings of the Physical Society. Section A, **68**, 1113 (1955).
[21] H.J. Goldsmid, H.B. Lyon, E.H. Volckmann. *Proc. 14th Int. Conf. on Thermoelectrics* (St. Petersburg, Russia, 1995) p. 16.
[22] R.S. Erofeev. Izv. Akad. Nauk SSSR, Neorg. Mater., **14**, 1422 (1978) (in Russian).
[23] O. Hellman, I.A. Abrikosov. Phys. Rev. B, **88**, 144301 (2013).
[24] O. Hellman, I.A. Abrikosov, S.I. Simak. Phys. Rev. B, **84**, 180301(R) (2011).
[25] Y. Xia, M.K.Y. Chan. Appl. Phys. Lett., **113**, 193902 (2018).
[26] L. Lindsay, A. Katre, A. Cepellotti, N. Mingo. J. Appl. Phys., **126**, 050902 (2019).